



**HAL**  
open science

# Robust optimization of horizontal drillstring rate of penetration through a nonlinear stochastic dynamic model

Americo Cunha Jr, Christian Soize, Rubens Sampaio

► **To cite this version:**

Americo Cunha Jr, Christian Soize, Rubens Sampaio. Robust optimization of horizontal drillstring rate of penetration through a nonlinear stochastic dynamic model. Biennial International Conference on Engineering Vibration (ICoEV-2015), Sep 2015, Ljubljana, Slovenia. pp.1-11. hal-01169135

**HAL Id: hal-01169135**

**<https://hal.science/hal-01169135>**

Submitted on 16 Sep 2015

**HAL** is a multi-disciplinary open access archive for the deposit and dissemination of scientific research documents, whether they are published or not. The documents may come from teaching and research institutions in France or abroad, or from public or private research centers.

L'archive ouverte pluridisciplinaire **HAL**, est destinée au dépôt et à la diffusion de documents scientifiques de niveau recherche, publiés ou non, émanant des établissements d'enseignement et de recherche français ou étrangers, des laboratoires publics ou privés.

## ROBUST OPTIMIZATION OF HORIZONTAL DRILLSTRING RATE OF PENETRATION THROUGH A NONLINEAR STOCHASTIC DYNAMIC MODEL

Americo Cunha Jr<sup>1,2,3</sup>, Christian Soize<sup>2</sup>, and Rubens Sampaio<sup>3</sup>

<sup>1</sup>Universidade do Estado do Rio de Janeiro  
americo@ime.uerj.br

<sup>2</sup>Université Paris-Est  
christian.soize@univ-paris-est.fr

<sup>3</sup>PUC–Rio  
rsampaio@puc-rio.br

**Keywords:** drillstring dynamics, horizontal drillstring, parametric probabilistic approach, robust optimization

**Abstract.** *A drillstring is a long column under rotation, composed by a sequence of connected drill-pipes and auxiliary equipment, which is used to drill the soil in oil prospecting. During its operation, this column presents a three-dimensional dynamics, subjected to longitudinal, lateral, and torsional vibrations, besides the effects of friction, shock, and bit-rock interaction. The study of the dynamics of this equipment is very important in many engineering applications, especially to reduce costs in the oil exploration process. In this sense, this work aims to formulate and solve a robust optimization problem that seeks to maximize horizontal drillstrings rate of penetration into of the soil, subjected to the restriction imposed by the structural limits of the column. To analyze the nonlinear dynamics of drillstrings in horizontal configuration, a computational model, which uses a nonlinear beam theory of Timoshenko type is considered. This model also takes into account the effects of friction and shock, induced by the lateral impacts between the drillstring and borehole wall, as well as bit-rock interaction effects. The uncertainties of the bit-rock interaction model are taken into account using a parametric probabilistic approach. Two optimizations problems (one deterministic and one robust), where the objective is to maximize the drillstring rate of penetration (ROP) into the soil, respecting its structural limits, are formulated and solved. In order to optimize the ROP, it is possible to vary the drillstring velocities of translation and rotation. The solutions of these optimization problems provided two different strategies to maximize the ROP.*

## 1 INTRODUCTION

The process of oil exploration involves very high costs, particularly during the drilling of a well. An effective way to reduce these costs is to optimize the drillstring rate of penetration into the soil, where a drillstring is a long column under rotation, composed by a sequence of connected drill-pipes and auxiliary equipment, which is used to drill the soil until the reservoir level. For this reason, and also because of the complex dynamics of this equipment, several recent studies have devoted attention to its study [12, 13, 1, 10, 4]. Some papers, in particular, focusing their attention on drillstrings in horizontal configuration, such as [14, 5, 11].

In the present work the objective is to formulate and solve a robust optimization problem that seeks to maximize horizontal drillstrings rate of penetration into of the soil, subjected to the restriction imposed by the structural limits of the column. For this purpose, a nonlinear beam theory of Timoshenko type is considered to analyze the nonlinear dynamics of drillstrings in horizontal configuration. Also, the mathematical model also takes into account the effects of friction and shock, induced by the lateral impacts between the drillstring and borehole wall, as well as bit-rock interaction effects. The uncertainties of the bit-rock interaction model are taken into account using a parametric probabilistic approach.

The rest of the paper is organized as follows. Section 2 presents the mathematical modeling of the nonlinear dynamics and the system efficiency analysis. In section 3 it is presented the probabilistic modeling of system parameters uncertainties. The formulation and solution of optimization problems that seek to maximize the drillstring rate of penetration into the soil can be seen in section 4. Finally, in section 5, the conclusions of the work are emphasized.

## 2 MODELING THE NONLINEAR DYNAMICS

### 2.1 Mechanical system of interest

The mechanical system of interest is sketched in Figure 1. It consists of a pair of stationary rigid walls, that emulates a horizontal rigid pipe, perpendicular to gravity acceleration  $g$ , which contains in its interior a deformable tube under rotation (rotating beam), subjected to three-dimensional displacements. This deformable tube has a length  $L$ , cross section area  $A$ , and is made of a material with mass density  $\rho$ , elastic modulus  $E$ , and shear modulus  $G$ . It loses energy through a mechanism of viscous dissipation, proportional to the mass operator, with damping coefficient  $c$ . Concerning the boundary conditions, the rotating beam is blocked for transversal displacements in both extremes; blocked to transversal rotations on the left extreme; and, on the left extreme, has a constant angular velocity around  $x$  equal to  $\Omega$ , and an imposed longitudinal velocity  $V_0$ .

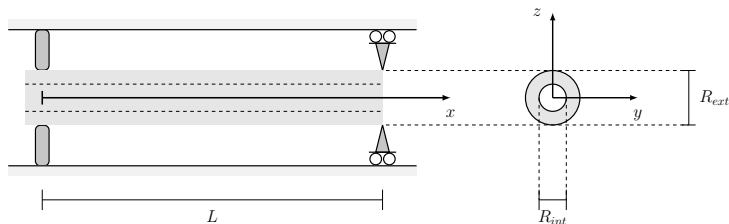


Figure 1: Schematic representation of the rotating beam which models the horizontal drillstring.

The beam theory adopted takes into account the rotatory inertia and shear deformation of beam cross section. Also, it is assumed that the beam is undergoing small rotations in the transverse directions, large rotation in  $x$ , and large displacements the three spatial directions, which couples the longitudinal, transverse and torsional vibrations.

In this way, the following kinematic hypothesis is adopted

$$\begin{aligned} u_x(x, y, z, t) &= u - y\theta_z + z\theta_y, \\ u_y(x, y, z, t) &= v + y(\cos\theta_x - 1) - z\sin\theta_x, \\ u_z(x, y, z, t) &= w + z(\cos\theta_x - 1) + y\sin\theta_x, \end{aligned} \quad (1)$$

where  $u_x$ ,  $u_y$ , and  $u_z$  respectively denote the displacement of a beam point in  $x$ ,  $y$ , and  $z$  directions, at the instant  $t$ . Also,  $u$ ,  $v$ , and  $w$  are the displacements of a beam neutral fiber point in  $x$ ,  $y$ , and  $z$  directions, respectively, while  $\theta_x$ ,  $\theta_y$ , and  $\theta_z$  represent rotations of the beam around the  $x$ ,  $y$ , and  $z$  axes respectively. Note that the physical quantities of interest are the fields  $u$ ,  $v$ ,  $w$ ,  $\theta_x$ ,  $\theta_y$ , and  $\theta_z$ , which depend on the position  $x$  and the time  $t$ .

## 2.2 Friction and shock effects

This beam is also able to generate shocks and friction effects in random areas of the rigid tube, which are described by the Hunt and Crossley shock model [7], and the standard Coulomb friction model [2].

The normal force of shock is given by

$$F_{\text{FS}}^n = -k_{\text{FS1}} \delta_{\text{FS}} - k_{\text{FS2}} \delta_{\text{FS}}^3 - c_{\text{FS}} |\delta|^3 \dot{\delta}_{\text{FS}}, \quad (2)$$

where  $k_{\text{FS1}}$ ,  $k_{\text{FS2}}$  and  $c_{\text{FS}}$  are constants of the shock model. The  $\dot{\cdot}$  is an abbreviation for time derivative, and the parameter  $\delta_{\text{FS}} = r - \text{gap}$ , where  $r = \sqrt{v^2 + w^2}$ , is dubbed *indentation*, and is a measure of penetration in the wall of a beam cross section, such as illustrated in Figure 2.

Once the column is rotating and moving axially, an impact also induces a frictional force in axial direction,  $F_{\text{FS}}^a$ , and a torsional friction torque,  $T_{\text{FS}}$ . Both are modeled by Coulomb friction law [2], so that

$$F_{\text{FS}}^a = -\mu_{\text{FS}} F_{\text{FS}}^n \text{sgn}(\dot{u}), \quad (3)$$

and

$$T_{\text{FS}} = -\mu_{\text{FS}} F_{\text{FS}}^n R_{bh} \text{sgn}(\dot{\theta}_x), \quad (4)$$

being  $\mu_{\text{FS}}$  the friction coefficient,  $\text{sgn}(\cdot)$  the sign function, and the radius of the borehole is  $R_{bh} = R_{ext} + \text{gap}$ .

## 2.3 Bit-rock interaction effects

At the beam right extreme act a force and a torque, which emulate the effects of interaction between the drill-bit and soil. They are respectively given by

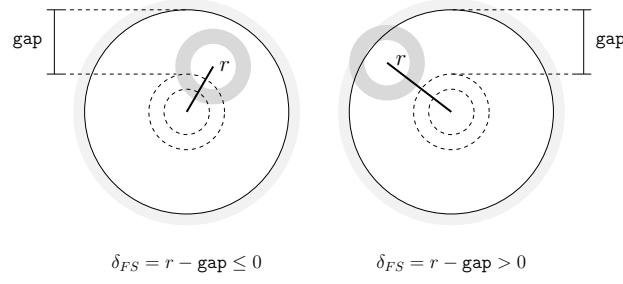


Figure 2: Illustration of indentation parameter in a situation without impact (left) or with impact (right).

$$F_{BR} = \begin{cases} \Gamma_{BR} \left( e^{-\alpha_{BR} \dot{u}_{bit}} - 1 \right) & \text{for } \dot{u}_{bit} > 0, \\ 0 & \text{for } \dot{u}_{bit} \leq 0, \end{cases} \quad (5)$$

and

$$T_{BR} = -\mu_{BR} F_{BR} R_{bh} \xi_{BR}(\omega_{bit}), \quad (6)$$

where  $\Gamma_{BR}$  is the bit-rock limit force;  $\alpha_{BR}$  is the rate of change of bit-rock force;  $\dot{u}_{bit} = \dot{u}(L, \cdot)$ ;  $\mu_{BR}$  bit-rock friction coefficient;  $\omega_{bit} = \dot{\theta}_x(L, \cdot)$ ; and  $\xi_{BR}$  is a regularization function. The expression for the bit-rock interaction models above were, respectively, proposed by [11] and [9].

## 2.4 Variational formulation of the nonlinear dynamics

Using a modified version of the extended Hamilton's principle, to include the effects of dissipation, one can write the weak equation of motion of the mechanical system as

$$\mathcal{M}(\boldsymbol{\psi}, \ddot{\mathbf{U}}) + \mathcal{C}(\boldsymbol{\psi}, \dot{\mathbf{U}}) + \mathcal{K}(\boldsymbol{\psi}, \mathbf{U}) = \mathcal{F}(\boldsymbol{\psi}, \mathbf{U}, \dot{\mathbf{U}}, \ddot{\mathbf{U}}), \quad (7)$$

where  $\mathcal{M}$  is the mass operator,  $\mathcal{C}$  is the damping operator,  $\mathcal{K}$  is the stiffness operator, and  $\mathcal{F}$  is the force operator. Also, the field variables and their weight functions are lumped in the vectors fields  $\mathbf{U} = (u, v, w, \theta_x, \theta_y, \theta_z)$ , and  $\boldsymbol{\psi} = (\psi_u, \psi_v, \psi_w, \psi_{\theta_x}, \psi_{\theta_y}, \psi_{\theta_z})$ . To see the definitions of the above operator the reader is referred to [8, 3].

The weak form of the initial conditions reads

$$\mathcal{M}(\boldsymbol{\psi}, \mathbf{U}(0)) = \mathcal{M}(\boldsymbol{\psi}, \mathbf{U}_0), \quad (8)$$

and

$$\mathcal{M}(\boldsymbol{\psi}, \dot{\mathbf{U}}(0)) = \mathcal{M}(\boldsymbol{\psi}, \dot{\mathbf{U}}_0), \quad (9)$$

where  $\mathbf{U}_0$  and  $\dot{\mathbf{U}}_0$ , respectively, denote the initial displacement, and initial velocity fields.

In order to simulate the nonlinear dynamics of the mechanical system, the physical parameters presented in Table 1 are adopted, as well as  $L = 100 \text{ m}$ , the rotational and axial velocities in x, respectively given by  $\Omega = 2\pi \text{ rad/s}$ , and  $V_0 = 1/180 \text{ m/s}$ .

Table 1: Physical parameters of the mechanical system that are used in the simulation.

parameter	value	unit
$\rho$	7900	$kg/m^3$
$g$	9.81	$m/s^2$
$\nu$	0.3	—
$\kappa_s$	6/7	—
$c$	0.01	—
$E$	$203 \times 10^9$	$Pa$
$R_{bh}$	$95 \times 10^{-3}$	$m$
$R_{int}$	$50 \times 10^{-3}$	$m$
$R_{ext}$	$80 \times 10^{-3}$	$m$

## 2.5 Discretization of the model equations

After the discretization of Eqs.(7), (8) and (9), by means of finite element method [6], one arrives the following initial value problem

$$[\mathcal{M}] \ddot{\mathbf{Q}}(t) + [\mathcal{C}] \dot{\mathbf{Q}}(t) + [\mathcal{K}] \mathbf{Q}(t) = \mathcal{F}(\mathbf{Q}, \dot{\mathbf{Q}}, \ddot{\mathbf{Q}}), \quad (10)$$

and

$$[\mathcal{M}] \mathbf{Q}(0) = \mathbf{Q}_0, \quad \text{and} \quad [\mathcal{M}] \dot{\mathbf{Q}}(0) = \dot{\mathbf{Q}}_0. \quad (11)$$

where  $\mathbf{Q}(t)$  is the generalized displacement vector,  $\dot{\mathbf{Q}}(t)$  is the generalized velocity vector,  $\ddot{\mathbf{Q}}(t)$  is the generalized acceleration vector,  $[\mathcal{M}]$  is the mass matrix,  $[\mathcal{C}]$  is the damping matrix,  $[\mathcal{K}]$  is the stiffness matrix, and  $\mathcal{F}$  is a nonlinear force vector, which contains contributions of an inertial force and a force of geometric stiffness.

The discretization of the structure uses a finite element mesh with 500 elements. As each element has 6 degrees of freedom per node, this results in a semi-discrete model with 3006 degrees of freedom. To reduce the computational cost of the simulations, the initial value problem of Eqs.(10) and (11) is projected in a vector space of dimension 49 to generate a reduced order model, which is integrated for the time interval  $[t_0, t_f] = [0, 10]$  s using the Newmark method [6], and the nonlinear system of algebraic equations, resulting from the time discretization, is solved by a fixed point iteration. Further details can be seen in [3].

## 2.6 Analysis of drilling process efficiency

The drilling process efficiency is defined as

$$\mathcal{E} = \frac{\int_{t_0}^{t_f} \mathcal{P}_{out} dt}{\int_{t_0}^{t_f} \mathcal{P}_{in} dt}, \quad (12)$$

where  $\mathcal{P}_{out}$  is the useful (output) power used in the drilling process, and  $\mathcal{P}_{in}$  is the total (input) power injected in the system. The output power is due to drill-bit movements of translation and rotation so that

$$\mathcal{P}_{out} = \dot{u}_{bit}^+ (-F_{BR})^+ + \omega_{bit}^+ (-T_{BR})^+, \quad (13)$$

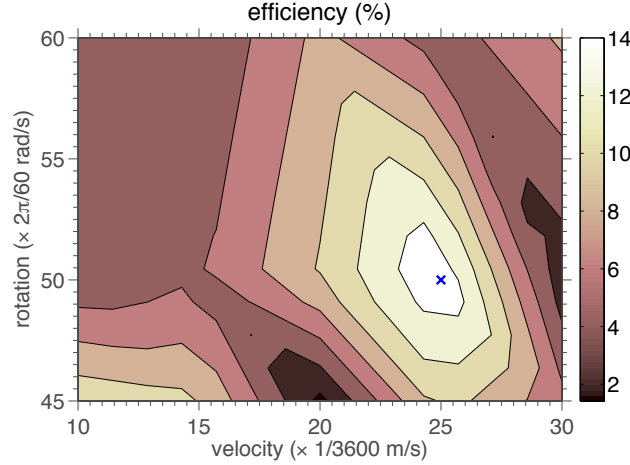


Figure 3: Illustration of efficiency function contour plot, for an “operating window” defined by  $1/360 \text{ m/s} \leq V_0 \leq 1/120 \text{ m/s}$  and  $3\pi/2 \text{ rad/s} \leq \Omega \leq 2\pi \text{ rad/s}$ . The maximum is indicated with a blue cross.

where the upper script  $+$  means the function positive part. The input power is defined as

$$\mathcal{P}_{in} = \dot{u}(0, t)^+ (-\lambda_1)^+ + \dot{\theta}_x(0, t)^+ (-\lambda_4)^+, \quad (14)$$

where the first and the fourth Lagrange multipliers, respectively, represent the drilling force and torque on the beam origin.

One can observe the contour map of  $\mathcal{E}$ , for an “operating window” defined by  $1/360 \text{ m/s} \leq V_0 \leq 1/120 \text{ m/s}$  and  $3\pi/2 \text{ rad/s} \leq \Omega \leq 2\pi \text{ rad/s}$ , in Figure 3.

Accordingly, it can be noted in Figure 3 that the optimum operating condition is obtained at the point  $(V_0, \Omega) = (1/144 \text{ m/s}, 5\pi/3 \text{ rad/s})$ , which is indicated with a blue cross in the graph. This point corresponds to an efficiency of approximately 16%. Suboptimal operation conditions occur in the vicinity of this point, and some points near the “operating window” boundary show lower efficiency.

### 3 MODELING OF SYSTEM-PARAMETER UNCERTAINTIES

The bit-rock interface law is given by Eqs.(5) and (6), so that this model is characterized by three parameters, namely,  $\alpha_{BR}$ ,  $\Gamma_{BR}$ , and  $\mu_{BR}$ . A parametric probabilistic approach [15, 16] is employed to construct the probabilistic model for each one parameter of these parameters, which are respectively modeled by random variables  $\mathcal{Q}_{BR}$ ,  $\mathbb{F}_{BR}$ , and  $\mathbb{J}_{BR}$ . In this approach, the maximum entropy principle is used to specify the probability distribution of the random parameters, taking into account only the known information about them.

For  $\mathcal{Q}_{BR}$ , it is assumed that

$$\int_{\alpha=0}^{+\infty} p_{\mathcal{Q}_{BR}}(\alpha) d\alpha = 1, \quad (15)$$

$$\mathbb{E}[\mathcal{Q}_{BR}] = m_{\mathcal{Q}_{BR}} > 0, \quad (16)$$

and

$$\mathbb{E}[\ln(\mathcal{Q}_{BR})] = q_{\mathcal{Q}_{BR}}, \quad |q_{\mathcal{Q}_{BR}}| < +\infty. \quad (17)$$

Thus, the maximum entropy distribution is given by

$$p_{\alpha_{\text{BR}}}(\alpha) = \mathbb{1}_{]0, \infty[}(\alpha) \frac{1}{m_{\alpha_{\text{BR}}}} \left( \frac{1}{\delta_{\alpha_{\text{BR}}}^2} \right)^{1/\delta_{\alpha_{\text{BR}}}^2} \times \frac{1}{\Gamma(1/\delta_{\alpha_{\text{BR}}}^2)} \left( \frac{\alpha}{m_{\alpha_{\text{BR}}}} \right)^{1/\delta_{\alpha_{\text{BR}}}^2 - 1} \exp\left( \frac{-\alpha}{\delta_{\alpha_{\text{BR}}}^2 m_{\alpha_{\text{BR}}}} \right), \quad (18)$$

which corresponds to the gamma distribution. Similar information are assumed to  $\Gamma_{\text{BR}}$ , so that this random variable also presents gamma distribution.

On the other hand, for the variable  $\mu_{\text{BR}}$  one assumes

$$\int_{\mu=0}^1 p_{\mu_{\text{BR}}}(\mu) d\mu = 1, \quad (19)$$

$$\mathbb{E} [\ln(\mu_{\text{BR}})] = q_{\mu_{\text{BR}}}^1, \quad |q_{\mu_{\text{BR}}}^1| < +\infty, \quad (20)$$

and

$$\mathbb{E} [\ln(1 - \mu_{\text{BR}})] = q_{\mu_{\text{BR}}}^2, \quad |q_{\mu_{\text{BR}}}^2| < +\infty, \quad (21)$$

which implies in a maximum entropy distribution of the form

$$p_{\mu_{\text{BR}}}(\mu) = \mathbb{1}_{[0,1]}(\mu) \frac{\Gamma(a+b)}{\Gamma(a)\Gamma(b)} \mu^{a-1} (1-\mu)^{b-1}, \quad (22)$$

that corresponds to the beta distribution.

For the probabilistic analysis of the dynamic system, the random variables of interest are characterized by the mean values  $m_{\alpha_{\text{BR}}} = 400 \text{ 1/m/s}$ ,  $m_{\Gamma_{\text{BR}}} = 30 \times 10^3 \text{ N}$ , and  $m_{\mu_{\text{BR}}} = 0.4$ , and the dispersion factors  $\delta_{\alpha_{\text{BR}}} = 0.5\%$ ,  $\delta_{\Gamma_{\text{BR}}} = 1\%$ , and  $\delta_{\mu_{\text{BR}}} = 0.5\%$ .

## 4 OPTIMIZATION OF THE RATE OF PENETRATION

### 4.1 Deterministic optimization problem

The instantaneous rate of penetration is given by the function  $\dot{u}_{bit}(t)$ , defined for all instants of analysis. Meanwhile, only contributes to the column advance, the positive part of this function  $\dot{u}_{bit}^+(t)$ . In addition, as objective function, it is more convenient to consider a scalar function. Thus, the temporal mean of  $\dot{u}_{bit}^+(t)$  is adopted as rate of penetration, and, consequently, objective function of the optimization problem

$$\text{rop}(\Omega, V_0) = \frac{1}{t_f - t_0} \int_{t=t_0}^{t_f} \dot{u}_{bit}^+(t) dt. \quad (23)$$

Furthermore, respect the material structural limits is indispensable to avoid failures in drillstring during the drilling process. For this reason, von Mises criterion of failure is considered, where it is established that, for all pairs  $(\Omega, V_0)$  in the “operating window”, one has

$$\text{UTS} - \max_{\substack{0 \leq x \leq L \\ t_0 \leq t \leq t_f}} \{ \sigma_{VM}(V_0, \Omega, x, t) \} \geq 0, \quad (24)$$

where UTS is the material ultimate tensile strength, and  $\sigma_{VM}$  is the von Mises equivalent stress.

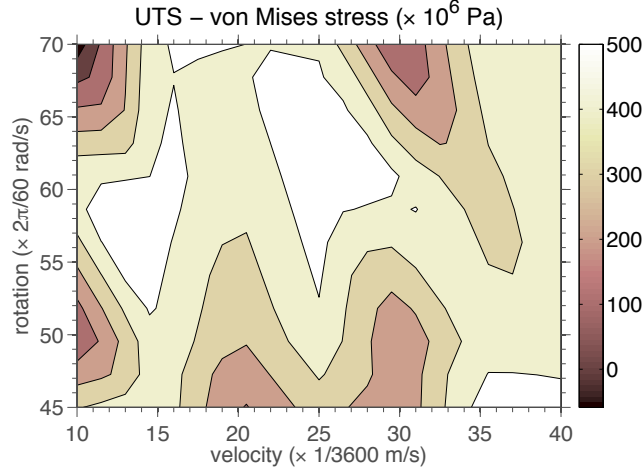


Figure 4: Illustration of maximum von Mises stress contour plot, for an “operating window” defined by  $1/360 \text{ m/s} \leq V_0 \leq 1/90 \text{ m/s}$  and  $3\pi/2 \text{ rad/s} \leq \Omega \leq 7\pi/3 \text{ rad/s}$ .

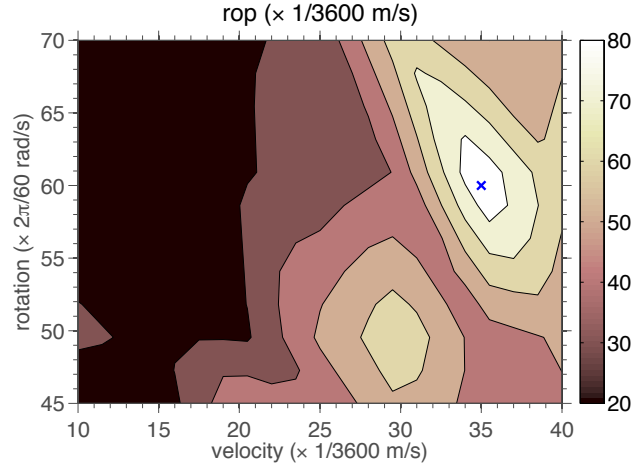


Figure 5: Illustration of rate of penetration function contour plot, for an “operating window” defined by  $1/360 \text{ m/s} \leq V_0 \leq 1/90 \text{ m/s}$  and  $3\pi/2 \text{ rad/s} \leq \Omega \leq 7\pi/3 \text{ rad/s}$ . The maximum is indicated with a blue cross.

Regarding the rate of penetration analysis, “operating window” is defined by the inequations  $1/360 \text{ m/s} \leq V_0 \leq 1/90 \text{ m/s}$  and  $3\pi/2 \text{ rad/s} \leq \Omega \leq 7\pi/3 \text{ rad/s}$ , and  $\text{UTS} = 650 \times 10^6 \text{ Pa}$ .

The contour map of constraint (24), is shown in Figure 4. From the way (24) is written, the Mises criterion is not satisfied when the function is negative, which occurs in a “small neighborhood” of the upper left corner of the rectangle that defines the “operating window”. It is noted that all other points respect the material structural limits. In this way, then, the “operating window” *admissible* region consists of all points that satisfy the constraint.

In Figure 5 the reader can see the contour map of *rop* function. Taking into account only points in the admissible region, the maximum of *rop* occurs at  $(V_0, \Omega) = (7/720 \text{ m/s}, 2\pi \text{ rad/s})$ , which is indicated on the graph with a blue cross. This point corresponds to a mean rate of penetration, during the time interval analyzed, approximately equal to 90 “meters per hour”.

## 4.2 Robust optimization problem

Taking into account the uncertainties, through the parametric approach presented in section 3, drill-bit velocity becomes the stochastic process  $\mathcal{U}_{bit}(t, \theta)$ , so that the random rate of penetration is defined by

$$\text{ROP}(V_0, \Omega, \theta) = \frac{1}{t_f - t_0} \int_{t=t_0}^{t_f} \dot{\mathcal{U}}_{bit}^+(t, \theta) dt. \quad (25)$$

In the robust optimization problem, who plays the role of objective function is the expected value of the random variable  $\text{ROP}(V_0, \Omega, \theta)$ , i.e.,  $\mathbb{E} [\text{ROP}(V_0, \Omega, \theta)]$ .

Regarding the restriction imposed by the von Mises criteria, now the equivalent stress is the random field  $\sigma_{VM}(V_0, \Omega, x, t, \theta)$ , so that the inequality is written as

$$\text{UTS} - \max_{\substack{0 \leq x \leq L \\ t_0 \leq t \leq t_f}} \{ \sigma_{VM}(V_0, \Omega, x, t, \theta) \} \geq 0. \quad (26)$$

However, the robust optimization problem considers as restriction a probability of the event defined by inequality (26),

$$\mathbb{P} \left\{ \text{UTS} - \max_{\substack{0 \leq x \leq L \\ t_0 \leq t \leq t_f}} \{ \sigma_{VM}(V_0, \Omega, x, t, \theta) \} \geq 0 \right\} \geq 1 - P_{risk}, \quad (27)$$

where  $0 < P_{risk} < 1$  is the risk percentage acceptable to the problem.

A robust optimization problem very similar to this one, in the context of a vertical drillstring dynamics, is considered in [13].

To solve this robust optimization problem it is employed a trial strategy which discretizes the “operating window” in a structured grid of points and then evaluates the objective function  $\mathbb{E} [\text{ROP}(V_0, \Omega, \theta)]$  and the probabilistic constraint (27) in these points.

Accordingly, it is considered the same “operating window” used in the deterministic optimization problem solved above, i.e.,  $1/360 \text{ m/s} \leq V_0 \leq 1/90 \text{ m/s}$  and  $3\pi/2 \text{ rad/s} \leq \Omega \leq 7\pi/3 \text{ rad/s}$ , in addition to  $\text{UTS} = 650 \times 10^6 \text{ Pa}$  and  $P_{risk} = 10\%$ . Each MC simulation in this case used 128 realizations to compute the propagation of uncertainties.

Concerning the simulation results, the probabilistic constraint (27) is respected in all grid points that discretize the “operating window”. Thus, the admissible region of robust optimization problem is equal to the “operating window”. In what follows, the contour map of function  $\mathbb{E} [\text{ROP}(V_0, \Omega, \theta)]$  can be see in Figure 6. Note that the maximum, which is indicated on the graph with a blue cross, occurs at the point  $(V_0, \Omega) = (1/90 \text{ m/s}, 7\pi/3 \text{ rad/s})$ . This point is located in the boundary of the admissible region, in the upper right corner, and corresponds to a expected value of the mean rate of penetration, during the time interval analyzed, approximately equal to 58 “meters per hour”.

This result says that, in the “operating window” considered here, increasing drillstring rotational and translational velocities provides the most robust strategy to maximize its ROP into the soil. This is in some ways an intuitive result, but is at odds with the result of the deterministic optimization problem, which provides another strategy to achieve optimum operating condition.

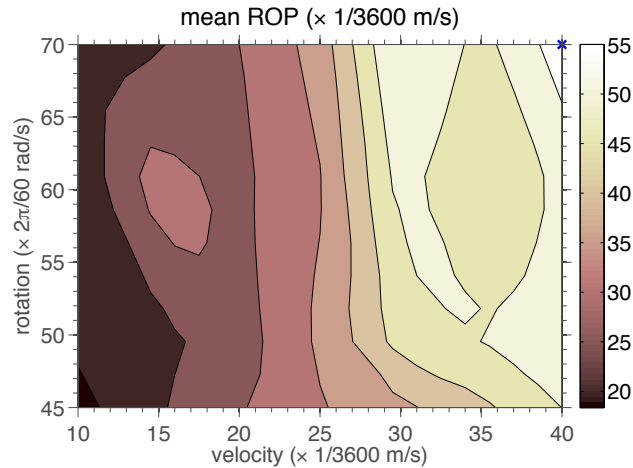


Figure 6: Illustration of the contour plot of the mean rate of penetration function, for an “operating window” defined by  $1/360 \text{ m/s} \leq V_0 \leq 1/90 \text{ m/s}$  and  $3\pi/2 \text{ rad/s} \leq \Omega \leq 7\pi/3 \text{ rad/s}$ . The maximum is indicated with a blue cross in the upper right corner.

## 5 CONCLUDING REMARKS

In this work a model that uses a beam theory, with effects of rotatory inertia and shear deformation, which is capable of reproducing large displacements effects, is employed to describe the nonlinear dynamics of horizontal drillstrings. This model also considers the friction and shock effects due to transversal impacts, as well as, the force and torque induced by bit-rock interaction. The uncertainties of the bit-rock interaction model were taken into account using a parametric probabilistic approach. A study aiming to maximize drilling process efficiency, varying drillstring velocities of translation and rotation was presented. The optimization strategy used a trial approach to seek for a local maximum, which was located within “operating window” and corresponds to an efficiency of approximately 16%. Two optimizations problems, one deterministic and one robust, where the objective was to maximize drillstring rate of penetration into the soil, respecting its structural limits, were formulated and solved. The solutions of these problems provided two different strategies to optimize the ROP.

## ACKNOWLEDGEMENTS

The authors are indebted to Brazilian agencies CNPq, CAPES, and FAPERJ, and French agency COFECUB for the financial support given to this research. The first author is grateful for the institutional support received from PUC-Rio and Université Paris-Est to carry out this work.

## REFERENCES

- [1] I. K. Chatjigeorgiou. Numerical simulation of the chaotic lateral vibrations of long rotating beams. *Applied Mathematics and Computation*, 219:5592–5612, 2013.
- [2] S. J. Cull and R. W. Tucker. On the modelling of Coulomb friction. *Journal of Physics A: Mathematical and General*, 32:2103–2113, 1999.

- [3] A. Cunha Jr. *Modeling and Uncertainty Quantification in the Nonlinear Stochastic Dynamics of a Horizontal Drillstrings*. D.Sc. Thesis, Pontificia Universidade Católica do Rio de Janeiro / Université Paris-Est, 2015.
- [4] A. Depouhon and E. Detournay. Instability regimes and self-excited vibrations in deep drilling systems. *Journal of Sound and Vibration*, 333:2019–2039, 2014.
- [5] Y. Hu, Q. Di, W. Zhu, Z. Chen, and W. Wang. Dynamic characteristics analysis of drillstring in the ultra-deep well with spatial curved beam finite element. *Journal of Petroleum Science and Engineering*, 82–83:166–173, 2012.
- [6] T. J. R. Hughes. *The Finite Element Method*. Dover Publications, New York, 2000.
- [7] K. H. Hunt and F. E. Crossley. Coefficient of restitution interpreted as damping in vibroimpact. *Journal of Applied Mechanics*, 42:440–445, 1975.
- [8] A. Cunha Jr, C. Soize, and R. Sampaio. Computational modeling of the nonlinear stochastic dynamics of horizontal drillstrings. (*submitted for publication*), 2015.
- [9] Y. A. Khulief, F. A. Al-Sulaiman, and S. Bashmal. Vibration analysis of drillstrings with self-excited stick–slip oscillations. *Journal of Sound and Vibration*, 299:540–558, 2007.
- [10] X. Liu, N. Vljajic, X. Long, G. Meng, and B. Balachandran. Nonlinear motions of a flexible rotor with a drill bit: stick-slip and delay effects. *Nonlinear Dynamics*, 72:61–77, 2013.
- [11] T. G. Ritto, M. R. Escalante, R. Sampaio, and M. B. Rosales. Drill-string horizontal dynamics with uncertainty on the frictional force. *Journal of Sound and Vibration*, 332:145–153, 2013.
- [12] T. G. Ritto, C. Soize, and R. Sampaio. Non-linear dynamics of a drill-string with uncertain model of the bit–rock interaction. *International Journal of Non-Linear Mechanics*, 44:865–876, 2009.
- [13] T. G. Ritto, C. Soize, and R. Sampaio. Robust optimization of the rate of penetration of a drill-string using a stochastic nonlinear dynamical model. *Computational Mechanics*, 45:415–427, 2010.
- [14] S. M. Sahebkar, M. R. Ghazavi, S. E. Khadem, and M. H. Ghayesh. Nonlinear vibration analysis of an axially moving drillstring system with time dependent axial load and axial velocity in inclined well. *Mechanism and Machine Theory*, 46:743–760, 2011.
- [15] C. Soize. *Stochastic Models of Uncertainties in Computational Mechanics*. Amer Society of Civil Engineers, Reston, 2012.
- [16] C. Soize. Stochastic modeling of uncertainties in computational structural dynamics — recent theoretical advances. *Journal of Sound and Vibration*, 332:2379–2395, 2013.